Journal of Biomaterials Science, Polymer Edition

Publication details, including instructions for authors and subscription information:
http://www.tandfonline.com/loi/tbsp20

Asymmetric Composite Membranes from Chitosan and Tricalcium Phosphate Useful for Guided Bone Regeneration

Hung-Yin Tai [a], Shiu-Huey Chou [b], Liao-Ping Cheng [a], Hung-Te Yu [a] & Trong-Ming Don [a]

[a] Department of Chemical and Materials Engineering, Tamkang University, Danshui District, New Taipei City, 25137, Taiwan

[b] Department of Life Science, Fu Jen Catholic University, Xinzhuang District, New Taipei City, 24205, Taiwan

Version of record first published: 08 May 2012.

To cite this article: Hung-Yin Tai , Shiu-Huey Chou , Liao-Ping Cheng , Hung-Te Yu & Trong-Ming Don (2012): Asymmetric Composite Membranes from Chitosan and Tricalcium Phosphate Useful for Guided Bone Regeneration, Journal of Biomaterials Science, Polymer Edition, 23:9, 1153-1170

To link to this article: http://dx.doi.org/10.1163/092050611X576657

VSP

Journal of Biomaterials Science 23 (2012) 1153–1170

Journal of BIOMATERIALS SCIENCE
brill.nl/jbs

Asymmetric Composite Membranes from Chitosan and Tricalcium Phosphate Useful for Guided Bone Regeneration

Hung-Yin Tai [a], **Shiu-Huey Chou** [b], **Liao-Ping Cheng** [a], **Hung-Te Yu** [a] **and Trong-Ming Don** [a,*]

[a] Department of Chemical and Materials Engineering, Tamkang University, Danshui District, New Taipei City 25137, Taiwan

[b] Department of Life Science, Fu Jen Catholic University, Xinzhuang District, New Taipei City 24205, Taiwan

Received 21 December 2010; accepted 25 April 2011

Abstract

To fulfill the properties of barrier membranes useful for guided bone tissue regeneration in the treatment of periodontitis, in this study a simple process combining lyophilization with preheating treatment to produce asymmetric barrier membranes from biodegradable chitosan (CS) and functional β-tricalcium phosphate (TCP) was proposed. By preheating TCP/CS (3:10, w/w) in an acetic acid solution at 40°C, a skin layer that could greatly increase the mechanical properties of the membrane was formed. The asymmetric membrane with a skin layer had a modulus value almost 4-times that of the symmetric porous membrane produced only by lyophilization. This is beneficial for maintaining a secluded space for the bone regeneration, as well as to prevent the invasion of other tissues. The subsequent lyophilization at −20°C then gave the rest of material an interconnected pore structure with high porosity (83.9–90.6%) and suitable pore size (50–150 μm) which could promote the permeability and adhesiveness to bone cells, as demonstrated by the *in vitro* cell-culture of hFOB1.19 osteoblasts. Furthermore, the TCP particles added to CS could further increase the rigidity and the cell attachment and proliferation of hFOB1.19. The TCP/CS asymmetric composite membrane thus has the potential to be used as the barrier membrane for guided bone regeneration.

Keywords

Chitosan, β-tricalcium phosphate, asymmetric membrane, guided bone regeneration

1. Introduction

Periodontitis has been widely regarded as a common disease of the periodontium which encircles and holds the teeth. It is caused by some inflammatory diseases that could destroy the periodontium. Serious periodontitis can result in a progressive retrograde of the alveolar bone. If this situation is not treated immediately, bone loss

* To whom correspondence should be addressed. Tel.: (886-2) 2629-3856; Fax: (886-2) 2621-9887; e-mail: tmdon@mail.tku.edu.tw

DOI:10.1163/092050611X576657

causes the periodontal pocket to deepen [1]. Bone defects resulting from disease are difficult to treat, because bone regenerates more slowly than other tissues and probably cannot be restored completely. Barrier membranes based on the guided tissue regeneration (GTR) technique have been used to overcome this problem [1–4]. The requirements of barrier membranes for successful treatments in periodontitis are as follows: selective permeability to prohibit the invasion of fibrous connective tissue, excellent bone affinity to guide bone regeneration, good mechanical strength to maintain a secluded space for bone regeneration, great adhesiveness between material and surrounding tissues to provide stability of membrane, and suitable degradability to prevent secondary surgery [3, 5–10]. Nowadays, non-degradable materials are widely used as barrier membranes, for example, polytetrafluoroethylene. However, these membranes must be removed at the second-stage operation after healing of the bone defect [3]. Comparatively, bioresorbable polymers [11, 12] are more advantageous for patients as they avoid the need for secondary surgery [3, 8]. Among these materials, chitosan (CS) is recognized as a potential GTR membrane material due to its excellent cell affinity, biodegradability and biocompatibility [7, 9, 13]. CS has been applied in various fields, including waste-water treatment, wound-healing dressing and controlled drug release [14–16]. CS gel and film have been proven to be useful for tissue engineering [5, 17, 18], in which they have been found to induce a minimal foreign body reaction. Most studies showed that, although in the short term a significant accumulation of neutrophils was found in the vicinity of CS implants, it dissipated rapidly and a chronic inflammatory response was not observed [14]. For example, Hamilton *et al.* [17] found that CS membranes could support high levels of osteoblast cell proliferation. Therefore, CS was chosen as the matrix material for GTR membrane in this study.

To further increase the bone affinity of CS membranes, the addition of other components for enhancing tissue regeneration has been investigated, such as growth factors, drugs or bioceramics [19–22]. In this study, calcium phosphate was used to improve the bone affinity of CS, since it has a chemical composition similar to bone. Calcium phosphate has excellent biological affinity and great interaction toward bone tissue; therefore, it has been widely investigated for applications in bone and dental implants [23–25]. Calcium phosphate has several forms of crystal structure. Among them, β-tricalcium phosphate (TCP), having a pure hexagonal crystal structure, has a suitable resorption rate which is very important for tissue regeneration [25, 26]. It has a moderate rate of dissolution in addition to its biocompatibility [26–28]. When osteoblasts are guided by Ca^{2+} and PO_4^{3-} released from TCP, the bone cells would be directed to mineralization. Therefore, it is considered as an ideal material which can be added to the CS membranes for enhancing bone tissue regeneration.

It is known that membranes with different structures and morphologies give rise to different cell attachment, proliferation and differentiation behaviors. To allow a high density of bone cells transforming to a new tissue, it would be better to have an interconnected pore structure with high porosity and suitable pore

size in the biodegradable membranes [27, 29]. Therefore, several methods, including non-solvent-induced phase separation, thermally-induced phase separation and porogen leaching methods, have been reported for creating such porous structures [29]. Lyophilization, in which the polymer solution is frozen to introduce phase separation [30], is simple. The solvent, generally water, is converted to the solid phase (i.e., ice) during the freezing process and simultaneously the polymer phase becomes concentrated. The polymer then forms a porous structure through the sublimation of ice by lyophilization. However, the as-prepared porous membranes generally have poor mechanical properties and mostly they are brittle. In addition, the membrane intended to be used in periodontal treatment not only serves as a template to guide bone regeneration but also a barrier to protect bone defects from the invasion of other tissues.

Some papers [29, 31, 32] have been published on calcium phosphate/CS composite membranes. Most researchers used hydroxyapatite, yet some others tried to incorporate β-tricalcium phosphate (β-TCP) into chitosan matrix to increase bone affinity and the proliferation of bone cells [31, 32]. For example, Liao *et al.* [31] demonstrated that a β-TCP/CS porous scaffold promoted human periodontal ligament cells associated with bone formation. The porous scaffold was a good candidate for periodontal tissue engineering. Kuo *et al.* [32] found that CS dense membranes incorporating β-TCP had a greater bone healing than the blank control after 4 weeks of recovery from a bone defect. Nearly all composite membranes used in previous studies were symmetric, i.e., completely dense membranes or completely porous membranes. In our study, on the contrary, an asymmetric β-TCP/CS membrane was fabricated and expected to be useful as the barrier membrane for guided bone tissue regeneration in the treatment of periodontitis. Moreover, this asymmetric membrane was prepared by a very simple method: preheating before lyophilization. By controlling the preheating time, a two-layer structure with suitable pore size and dense surface was achieved. The porous layer was expected to provide a good environment for the growth of osteoblasts, and the dense layer could prevent the invasion of other tissues in addition to give better mechanical properties as shown in Fig. 1. Thus, different barrier membranes were prepared by changing the preheating time. Their structures and properties were then investigated. In ad-

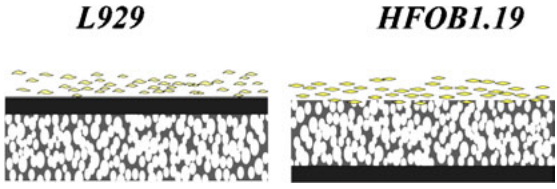

Figure 1. A cartoon picture for the illustration of L929 fibroblast cultured on the top surface (skin layer) and hFOB1.19 bone cells on the bottom surface (porous layer) of the membranes. This figure is published in colour in the online edition of this journal, which can be accessed *via* http://www.brill.nl/jbs

dition, osteoblasts (hFOB1.19) were cultured on these membranes *in vitro* to test their bone affinity.

2. Materials and Methods

2.1. Materials

Chitosan (CS) was purchased from Tokyo Chemical. For purification, CS flasks were dissolved in a 2% acetic acid solution by continuously stirring for 24 h at 50°C. The solution was then filtered to remove any insoluble impurities. The filtrate was poured into a NaOH solution (1 M), resulting in white CS precipitate. The precipitate was washed by double-distilled water until the pH value of filtrate reached 7. The product was dried by lyophilization at −20°C and crushed into powder. After purification, the molecular weight of CS decreased from 450 to 350 kg/mol, as determined by a viscosimetry; yet, the degree of deacetylation did not change and had a value of 86%, as measured by UV spectrophotometry, as well as by NMR [33–35]. Moreover, the endotoxin level of the purified CS was decreased from original 1.0 to 0.6 EU/mg. β-Tricalcium phosphate (TCP, Acros Organics) was ground by a ball-mill to a final size of 2.0 ± 0.3 μm as determined by a particle size analyzer (Zetasizer).

2.2. Preparation of Asymmetrical Composite Membranes

A 2 wt% CS solution was first prepared by dissolving a specific amount of CS in a 0.5% (w/v) acetic acid aqueous solution. TCP particles (3.0 g TCP based on 10.0 g CS) were then added into the CS solution. The TCP/CS mixture was stirred at 50°C for 9 h. Two asymmetrical membranes, TCPCS-20 and TCPCS-40, were obtained by first preheating the mixture in a ventilation oven at 40°C for 20 and 40 min, respectively, and followed by lyophilization at −20°C. Both membranes were neutralized with a basic solution, NaOH(aq), and then washed with a great amount of distilled water until pH 7 was reached. A symmetric porous membrane TCPCS-0 was prepared by direct lyophilization at −20°C without any preheating treatment. For comparison, CS membranes without TCP were also prepared with the same procedure where CS-0 was the symmetric porous membrane, and CS-20 and CS-40 were the asymmetric membranes with the preheating time of 20 and 40 min, respectively.

2.3. Morphology and Structure of the Composite Membranes

The morphology of composite membranes was examined using a scanning electron microscope (SEM, S-2600H, Hitachi). To observe the cross-section, membranes were fractured in the liquid nitrogen. Samples were sputtered by a very thin layer of gold and images were then taken by the SEM. An X-ray diffractometer (D8-Advance, Bruker) employing the Cu-Kα radiation was used to examine the crystal structures of TCP and CS. The diffractometer was operated at 45 kV and 40 mA over the 2θ range of 5–55° for the TCP powder and composite membranes.

The bulk porosity was defined as the fraction of pore volume in the membrane and was determined using the liquid displacement method [36], in which ethanol was used as the liquid phase. The membrane was first immersed in a specific volume of ethanol (V_0) in a graduated cylinder. After immersion, the ethanol was then forced into the pores of the membrane *via* a series of brief evacuation–repressurization cycles. Cycling was continued until no air bubbles were observed emerging from the membrane. The volume reading, V_1, indicated the total volume of free ethanol and the membrane being impregnated with ethanol. The impregnated membrane was then removed from the cylinder, and the volume of residual free ethanol was recorded as V_2. The volume difference $V_1 - V_2$ was the volume of the membrane, whereas the quantity $V_0 - V_2$ was the ethanol volume held in the membrane, i.e., the pore volume within the membrane. The bulk porosity of the membrane was then expressed as:

$$\text{Bulk porosity } (\%) = \left(\frac{V_0 - V_2}{V_1 - V_2}\right) \times 100. \quad (1)$$

The averages and SD values were determined from five measurements. In addition, the surface porosity was calculated as the surface void area divided by the total surface area using Image-Pro Plus software (Media Cybernetics), the average values and standard deviations were determined from five different SEM images.

2.4. Dynamic Storage Modulus

The storage modulus of the composite membranes was measured with a dynamic mechanical analyzer (TA Q800) using the tension mode. Rectangular samples with a width of 6.5 mm and a length of 30 mm were prepared. The frequency was set at 1 Hz and the heating rate was 3°C/min from 30 to 150°C.

2.5. Water Absorption of Composite Membranes

For the water absorption experiment, circular membranes with a diameter of 1.5 cm were cut out. The membrane was dried first in a vacuum oven at 50°C until it reached a constant weight, W_0. It was than immersed in Ringer's solution (Sigma) at pH 7.4 and 37°C. After immersion for a specific time interval (2–28 h), the wet membrane was removed and gently wiped with a lens-cleaning tissue to remove the free water from the surface. It was then weighed again (W_t). The water absorption in percentage, M_t (%), was calculated according to the following equation:

$$M_t\ (\%) = \left(\frac{W_t - W_0}{W_0}\right) \times 100. \quad (2)$$

The results were obtained by taking the average of three determinations.

2.6. Enzymatic Degradability of Composite Membranes

The enzymatic degradability of composite membranes was conducted by immersing the membranes in Ringer's solution which was added additionally with

0.5 mg/ml lysozyme (Sigma) and 2 mg/ml amylase (Sigma) to simulate the environment of the oral cavity [37]. In addition, NaN_3 was added to inhibit the bacteria growth. The samples were incubated in a shaker set at 60 rpm and 37°C. After 7 days of incubation, the membranes were removed and weighed. The degradability of the membranes was then represented by their weight loss percentage. The morphology of the membranes after degradation was also examined using SEM.

2.7. In Vitro *Cell Compatibility*

Mouse fibroblast-like cells (L929) were suspended in DMEM (Gibco/Invitrogen) supplemented with 10% FBS (Gibco/Invitrogen). Human osteoblast cells (hFOB1.19) were suspended in DMEM/F12 (Gibco/Invitrogen) supplemented with 10% FBS. Cells were cultured in a humidified atmosphere of 95% air and 5% CO_2 at 37°C. Medium was renewed every 2 days. The membranes were placed into tissue-culture treated polystyrene plates and fixed by silicone rings. The L929 cells were cultured on the surface skin layer, whereas the hFOB1.19 cells were cultured on the porous layer of the composite membranes (see Fig. 1). The L929 and hFOB1.19 were suspended in the culture medium at 5×10^4 and 2×10^4 cells/ml, respectively.

The proliferation of L929 and hFOB1.19 was determined from the cell viability using the methylthiazol tetrazolium (MTT) assay (Sigma) over a period of 4 days. At a specific time interval, 150 µl MTT was pipetted into each well and incubated for 3 h at 37°C. The viable cells would turn the yellow reagent to a blue formazan. Following, 200 µl isopropanol containing 0.06 M HCl was added to dissolve the insoluble formazan. The absorbance of the colored solution was measured by enzyme-linked immunosorbent assay (ELISA) at 570 nm. The cell number was then estimated from the standard calibration curve.

3. Results and Discussion

3.1. Membrane Preparation and Characterization

In this study, composite membranes with different structures were prepared from the biodegradable CS and functional TCP. CS was used as the matrix of membranes, not only providing the surface for cell attachment but also maintaining a space for tissue reconstruction. TCP is composed of Ca^{2+} and $PO_4{}^{3-}$, and, therefore, it is important in guiding bone tissue regeneration.

For preparing skinless porous membranes, the CS solution and the TCPCS mixture were directly frozen and lyophilized to obtain the respective CS-0 and TCPCS-0 symmetric porous membrane. Representative microstructures of CS-0 and TCPCS-0 illustrating a highly porous yet interconnected structure are presented in Fig. 2. Pore size distribution is observed for both CS-0 and TCPCS-0 membranes with pore size ranging from 50 to 150 µm. In addition, the TCP particles can be clearly seen on the SEM micrographs of the TCPCS-0 membrane. These particles had an average size of 2.0 ± 0.3 µm and were uniformly distributed in the CS ma-

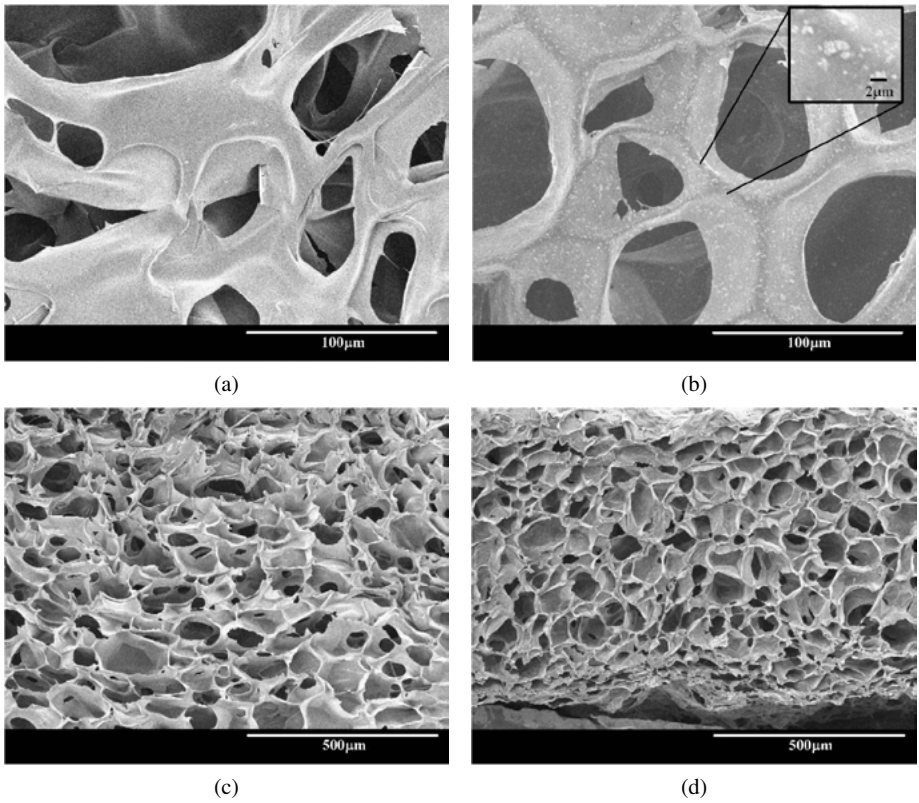

(a) (b)

(c) (d)

Figure 2. SEM micrographs of the top surface: (a) CS-0, (b) TCPCS-0; and the cross-section: (c) CS-0, (d) TCPCS-0. The scale bar for (a) and (b) is 100 μm, and the scale bar for (c) and (d) is 500 μm. The TCP particles had an average size of 2.0 ± 0.3 μm and was uniformly distributed in the TCPCS membrane as indicated in panel (b).

trix. If the CS solution was preheated in the oven at 40°C for a period of time before freezing, the morphology of membranes could be changed. If the preheating time was controlled to avoid a complete drying of the CS solution, it is possible to form a skin layer on the surface due to the faster evaporation of solvent at the surface. Beneath the skin layer, it would be still a polymer solution. The formation of a skin layer and its thickness, thus, could be controlled by the preheating time. After preheating, the solution with a skin layer was then frozen and lyophilized to form an asymmetric membrane composed of a skin layer and a porous sub-layer. Figures 3 and 4 show the SEM micrographs of the as-prepared asymmetric membranes with a preheating time of 20 and 40 min, respectively. From the images, it can be seen that the surface porosity decreased with increasing the preheating time. The porosity values of various membranes are listed in Table 1. For the membranes prepared with 20-min preheating, CS-20 and TCPCS-20, there were still some voids on the top surface. The top surface porosity was 20.5% for the CS-20 membrane and 18.8% for the TCPCS-20 composite membrane. After increasing the preheating time to 40 min, a dense skin layer was formed on the top surface for both CS and

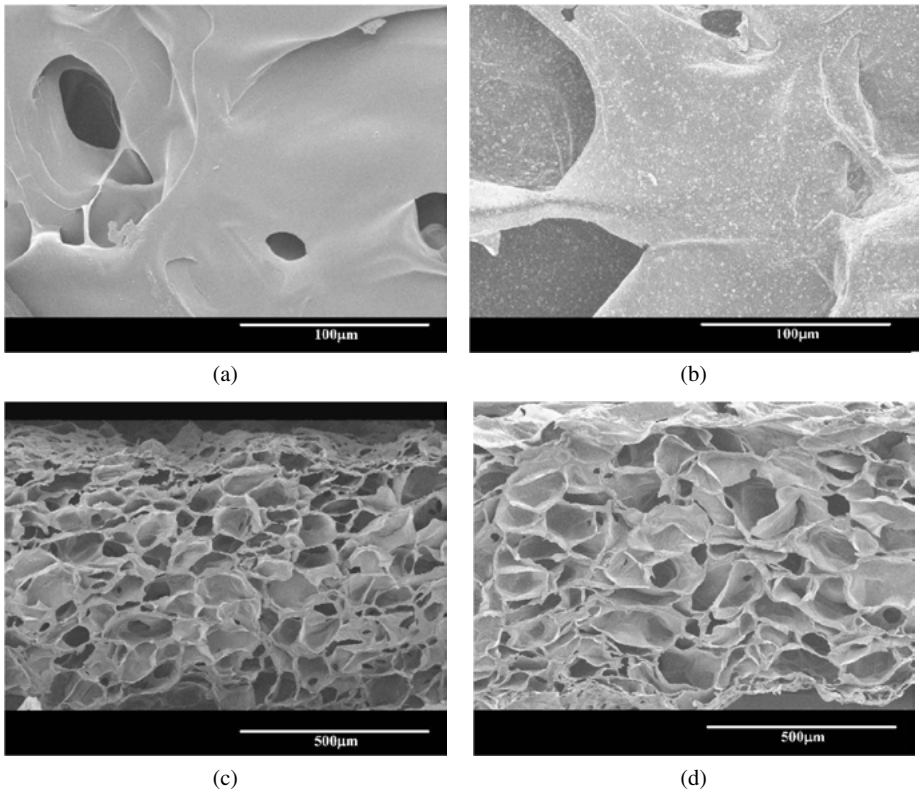

Figure 3. SEM micrographs of the top surface: (a) CS-20, (b) TCPCS-20; and the cross-section: (c) CS-20, (d) TCPCS-20. The scale bar for (a) and (b) is 100 μm, and the scale bar for (c) and (d) is 500 μm.

TCPCS membranes, as shown in Fig. 4. Just as the membrane formed without preheating, the TCP particles were found to be distributed uniformly in the CS matrix. In the same figure, the cross-section of the CS-40 and TCPCS-40 membranes shows a porous structure beneath the skin layer, indicating the successful preparation of an asymmetric structure. Yet, the cross-section image reveals that the thickness of the membrane decreased with an increase in the preheating time as listed in Table 1. The bulk porosity of membranes prepared with different preheating times was also measured. There was a slight decrease in the bulk porosity with the preheating time. This is because the preheating process would evaporate the water to some extent depending on the heating time and, thus, decrease the amount of water in the solution. Subsequently, the water in the solution was frozen to ice and the CS then formed a porous structure through the sublimation of ice by lyophilization. The higher amount of the water in the original solution, the higher the porosity of the membrane is. Therefore, increasing the preheating time would decrease the amount of water and in turn decrease the porosity of the prepared membrane. Nevertheless, the membranes with such porosities, 84–93%, are still suitable for the GTR. The bottom surface porosity also decreased with the preheating time, yet the de-

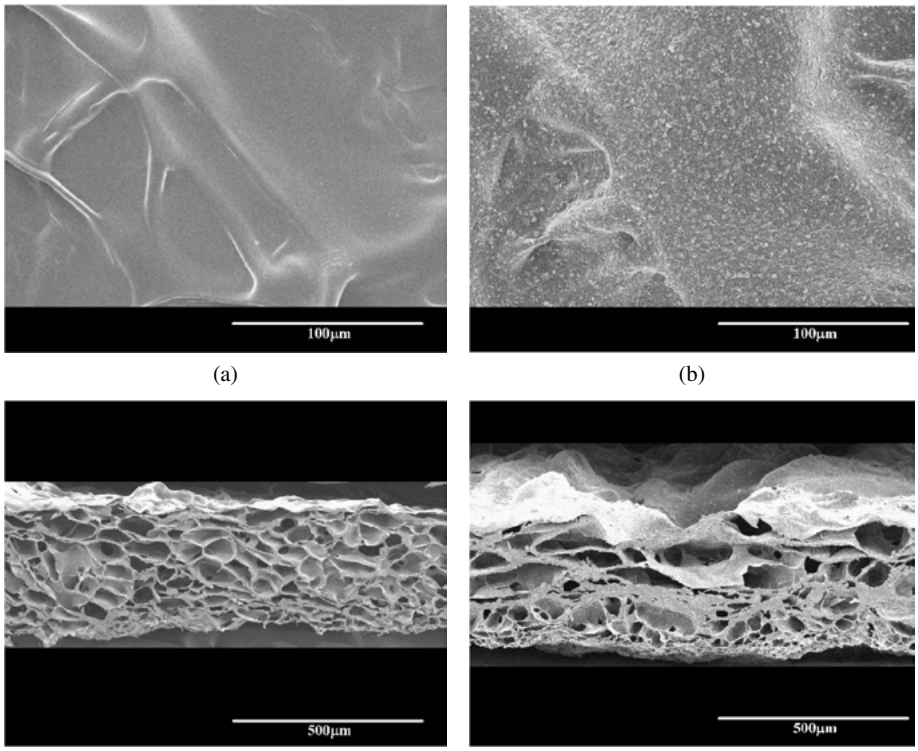

Figure 4. SEM micrographs of the top surface: (a) CS-40, (b) TCPCS-40; and the cross-section: (c) CS-40, (d) TCPCS-40. The scale bar for (a) and (b) is 100 μm, and the scale bar for (c) and (d) is 500 μm.

Table 1.
Characteristics of the CS and TCPCS membranes prepared with different preheating times before lyophilization

	Preheating time (min)	Thickness (μm)	Surface porosity (top, %)	Surface porosity (bottom, %)	Bulk porosity (%)
CS-0	0	1228 ± 62	40.1 ± 2.5	48.9 ± 3.1	92.9 ± 0.5
CS-20	20	702 ± 19	20.5 ± 2.4	42.3 ± 1.3	87.5 ± 2.6
CS-40	40	394 ± 55	1.5 ± 0.2	40.4 ± 2.0	84.6 ± 1.7
TCPCS-0	0	1117 ± 54	38.9 ± 2.7	46.2 ± 2.4	90.6 ± 1.2
TCPCS-20	20	813 ± 53	18.8 ± 2.1	42.5 ± 2.0	87.2 ± 1.4
TCPCS-40	40	317 ± 37	1.2 ± 0.1	39.2 ± 2.4	83.9 ± 0.2

The surface porosity was calculated as the void area divided by the total surface area using Image-Pro Plus software (Media Cybernetics). The bulk porosity was determined by using liquid displacement method, and EtOH was used as the liquid phase.

crease was small. The reason is the same for the decrease of the bulk porosity. The bottom surface of the asymmetric membranes prepared with 40 min of preheating before lyophilization (CS-40 and TCPCS-40) still had porosity values around 40%.

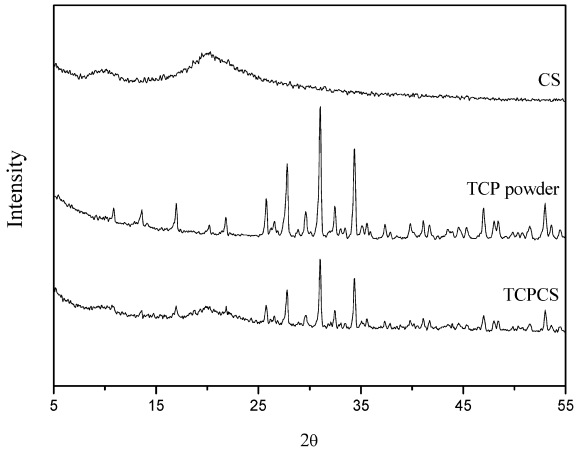

Figure 5. XRD patterns of the CS-0, TCP powder and TCPCS-0 composite membrane.

It can also be seen from Table 1 that the addition of TCP particles did not affect the porosity of membranes significantly.

The crystalline structure of the prepared membranes was confirmed by X-ray diffraction. Figure 5 shows the XRD patterns for CS-0, TCP and TCPCS-0. For CS, two broad peaks centered at about $2\theta = 10.1°$ and 20.25° were observed [19, 38]. As TCP was added into CS, these two characteristic peaks became flatter, implying that the addition of TCP could result in a decrease of the crystallinity of the CS matrix. During the preparation, the presence of TCP would be anticipated to weaken the intermolecular interactions of CS, thereby reducing its crystallinity. Yet, sharp diffraction peaks located at around 31.7°, 34.1° and 25.9°, corresponding to the respective (211), (202) and (002) planes of TCP, were still observed from the composite membranes, indicating that the structure of TCP did not change during the preparation of composite membranes. Similar behaviors were observed for the asymmetric composite membranes prepared with the preheating treatment before lyophilization.

3.2. Storage Modulus of Composite Membranes

The storage modulus of different membranes was measured with a dynamic mechanical analyzer and the results are shown in Fig. 6. It can be seen that the composite membranes with the addition of TCP rigid particles had higher storage modulus than their respective CS membranes without TCP. By adding 30 phr of TCP particles, the modulus increased by 81% for the symmetric porous membrane without preheating, and by 272% for the asymmetric membrane prepared with 40 min of preheating before lyophilization. The results also demonstrate that the preheating process before lyophilization had a significant effect on the storage modulus of the membrane. Increasing the preheating time increased the storage modulus of the membrane, which was more obvious for the TCPCS composite membranes. The TCPCS-40 membrane prepared with 40 min preheating had a modulus almost 4-

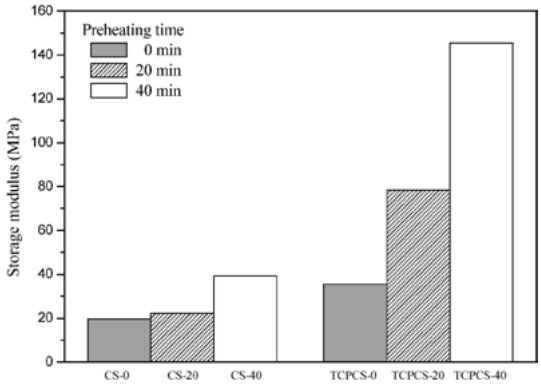

Figure 6. Storage modulus at 25°C of the CS and TCPCS membranes prepared with different preheating times before lyophilization.

times that of the TCPCS-0 without preheating. This can be explained by the fact that increasing the preheating time helps the formation of a dense skin layer and the decrease of porosity. The skin layer, thus, plays a critical role in the mechanical properties of membranes. It is thus possible to control the mechanical properties of the membranes by varying the preheating time before lyophilization.

3.3. Water Absorption and Enzymatic Degradation

Although CS can dissolve in an acidic solution due to the protonation of amino groups, it is not easily swollen in neutral water because of inter- and intra-molecular hydrogen bonding from its hydroxyl and amino groups. However, the water absorption greatly depends on the porosity of the membrane. For example, a dense CS membrane prepared after complete drying in the oven can only have equilibrium water absorption of 270% in the Ringer's solution at pH 7.4 and 37°C. The equilibrium water absorption increases greatly to almost 1720% for a porous CS membrane prepared by direct lyophilization. The water absorption of CS and its composite membranes prepared with different preheating times were thus measured in the Ringer's solution at pH 7.4 at 37°C. It can be seen in Fig. 7 that the water absorption in most membranes increased rapidly in the first 2 h and thereafter it increased slowly. After 8 h of immersion, most membranes reached their equilibrium absorption values. Figure 7 also shows that increasing the preheating time decreased the water absorption of the membrane because of the gradual formation of the skin layer and the decrease of porosity. This is true for both CS and TCPCS membranes. The asymmetric CS membrane with a skin layer (CS-40) had the final water absorption of 900%, only about one-half of the porous symmetric membrane CS-0. The addition of TCP can further decrease the water absorption of the membrane as evidenced by the comparison of Fig. 7a and b. This is mainly because the TCP particles could not absorb any water.

The choice of CS as the matrix of composite membranes is based on the advantage of its biodegradability. To investigate its suitability as bone regeneration mate-

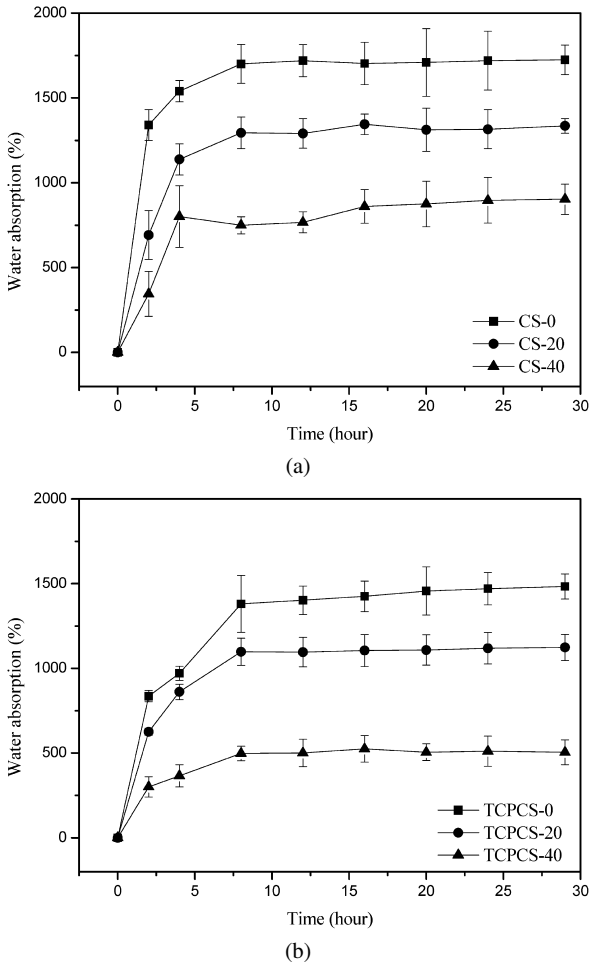

Figure 7. Water absorption of the (a) CS and (b) TCPCS membranes prepared with different preheating times before lyophilization. CS-0 and TCPCS-0: without preheating, CS-20 and TCPCS-20: 20 min of preheating; CS-40 and TCPCS-40: 40 min of preheating.

rials, *in vitro* degradation of the composite membranes was measured. The extent of degradation of the CS and TCPCS composite membranes after 7 days of immersion in Ringer's solution containing lysozyme and amylase to simulate the environment of oral cavity is shown in Fig. 8. It is clear that all membranes were degradable, and the TCPCS membranes had lower weight loss than the CS membranes. Even the TCP particles were assumed to be insoluble and non-degradable, and the weight-loss calculation was only based on the original weight of CS component, the values were still lower for the TCPCS membranes. Two possible explanations are proposed to explain the lower weight loss in the TCPCS composite membranes. First, since enzymes are water-soluble, the decrease in the water absorption by the addition of TCP particles could probably decrease the enzymatic degradability. Second, it is very likely that the TCP particles in the CS matrix could affect the binding of

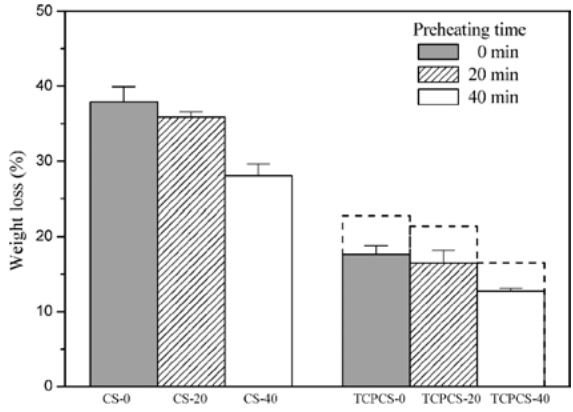

Figure 8. Enzymatic degradability of the CS and TCPCS membranes after immersion in Ringer's solution for 7 days. The Ringer's solution contained 0.5 mg/ml lysozyme and 2 mg/ml amylase. The dashed lines in the TCPCS group indicate that the calculation of weight loss percentage was only based on the original weight of CS component.

enzymes on the CS, thereby decreasing the degradability. However, this needs further investigation. Furthermore, the morphology of membranes controlled by the preheating time could also have effects on the degradable properties. The asymmetric membranes with a skin layer were degraded slower than the symmetric porous membranes. Increasing the preheating time decreased the degradation extent of the membrane. For the asymmetric membrane with a skin layer (CS-40 or TCPCS-40), the weight loss after 1 week was about 25% less than that of the corresponding symmetric porous membranes (CS-0 or TCPCS-0). The existence of a skin layer and the lower porosity in the asymmetric membranes caused the decrease in the degradation rate. The top surface of membranes after 7 days of degradation was examined by SEM. From Fig. 9 it can be seen that the interconnected hatches among pores were severely cleaved due to the action of enzymes. In addition, the images show that the degradation extent was more obvious for the CS membrane than the corresponding TCPCS composite membrane with the same preheating time, in agreement with the weight-loss results. The above results, therefore, imply that the addition of TCP particles and the preheating process could prolong the degradation time of membranes. Since complete bone regeneration takes about 6–8 weeks it would be better that the barrier membrane has the same time-scale in degradation. Further experiments show that the TCPCS-40 asymmetric membrane had a weight loss value of 82–93% after 6 weeks, which is suitable to be used as the barrier membrane for GTR in the periodontitis.

3.4. Cytotoxicity of the CS and TCPCS Membranes

Cytotoxicity analysis using MTT assay has been widely used as the preliminary investigation for cell compatibility of materials. The biological analysis provides information whether or not the material will induce any cytotoxicity on the cells. Here, the MTT assay was employed to evaluate the cell viability of L929 cells cul-

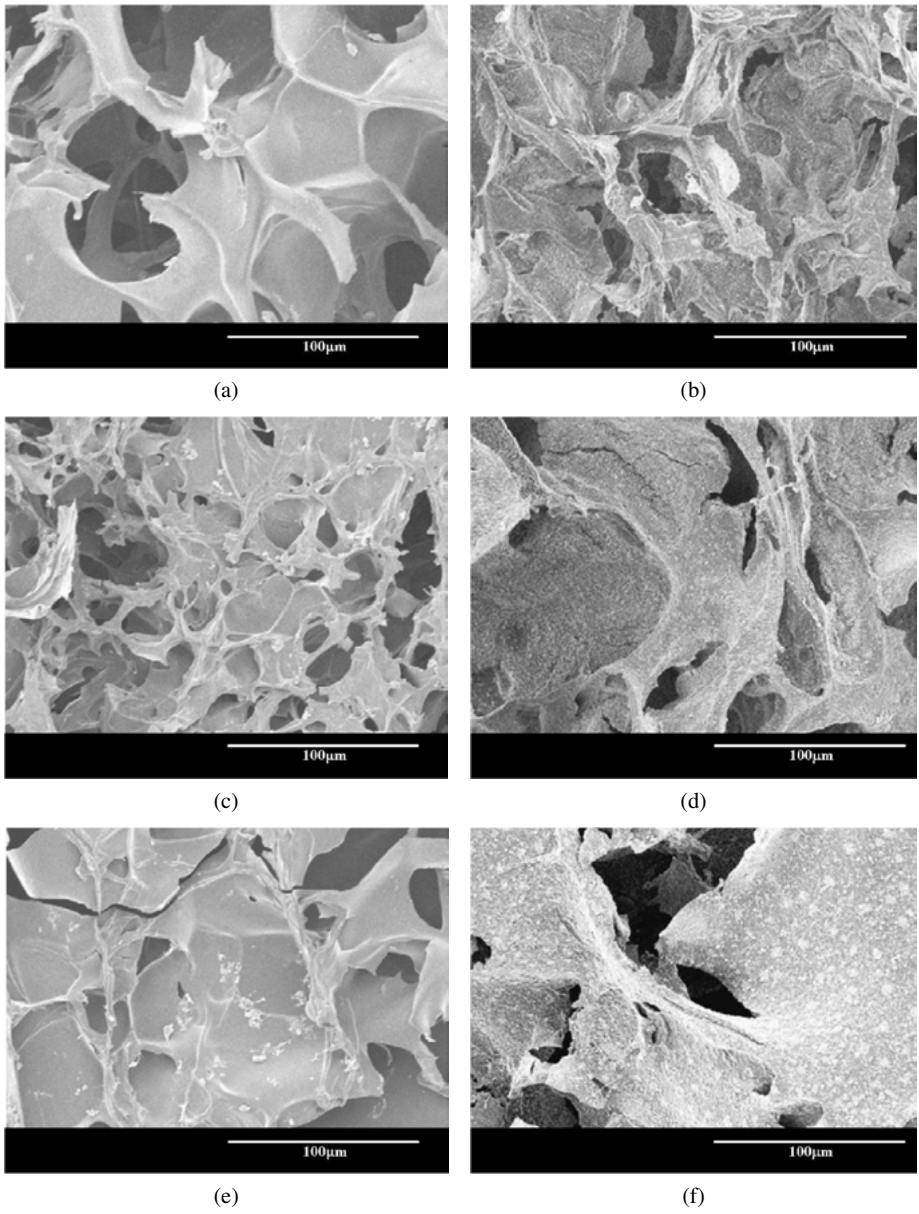

Figure 9. SEM micrographs of the top surface of (a) CS-0, (b) TCPCS-0, (c) CS-20, (d) TCPCS-20, (e) CS-40 and (f) TCPCS-40 after 7 days of enzymatic degradation. The scale bar is 100 μm.

tured on the top surface of various membranes as shown in Fig. 10. The control group was L929 cells cultured on a blank tissue-culture treated plate. It was confirmed that the CS membranes and TCPCS composite membranes did not cause any cytotoxic effect to L929 cells. All membranes had almost the same cell viability as the control on day 4. This also implies that the TCP particles added in the

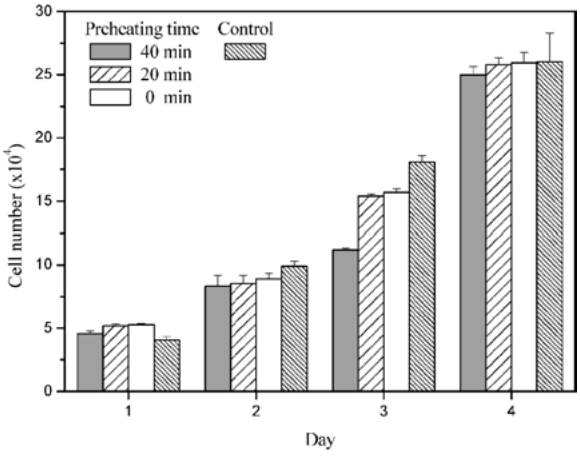

(a)

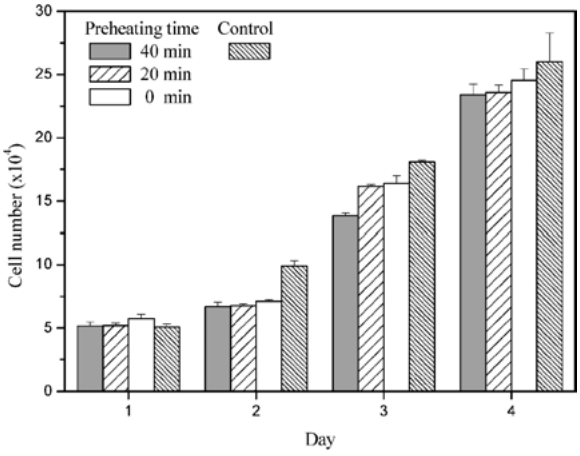

(b)

Figure 10. Cell viability of L929 cells cultured on the top surface of (a) CS membranes and (b) TCPCS membranes during 4 days. The membranes were prepared with different preheating times before lyophilization.

CS membranes did not impose any negative effects on the cell compatibility. In addition, Fig. 10 shows that the asymmetric membranes with a skin layer (CS-40 and TCPCS-40) had lower cell viability than the corresponding membranes with a porous surface (CS-0 and TCPCS-0) in the first three days; yet, the differences were not large, and even were insignificant on day 4. Therefore, the results imply that the fibroblast cells could also proliferate well on the skin layer of the CS-40 and TCPCS-40 membranes, at least 96% and 90% of the control on day 4, respectively.

3.5. Proliferation of hFOB1.19 Cells on the CS and TCPCS Membranes

The cell proliferation of hFOB1.19 cells cultured on the bottom surface of various membranes during a period of 4 days is shown in Fig. 11. There are no significant

differences in the cell number with respect to the preheating times on day 1. It indicates that the cell attachment on the porous layer of membranes was similar when their surface porosities were close. Table 1 shows that the bottom surface porosities were in the range of 40.4–48.9% for the CS membranes and 39.2–46.2% for the TCPCS membranes. Following, the hFOB1.19 grew rapidly and reached a plateau value after 3 days of cell culture. However, the membrane prepared with a longer preheating time had lower cell viability toward hFOB1.19 on day 2 and day 3, as can be seen in Fig. 11. This is because the porosity of the membrane decreased with increasing the preheating time (see Table 1), though they were all porous. However, the differences were small. Therefore, the preheating process is still acceptable for the osteoblast cells to proliferate on the bottom surface of the membranes, especially when TCP particles are added into the membranes. The effect of the addition of TCP powder can be seen by comparing Fig. 11a and b. The hFOB1.19 proliferated much better on the TCPCS membranes than on the CS membranes. The cell number on day 4 increased by about 20% for the TCPCS membrane when compared with the corresponding CS membrane with the same preheating time. This proves the positive effect of the addition of TCP particles on bone cell proliferation. The TCP can provide a template for the growth of osteoblasts. In addition, the steady and gradual dissolution of TCP particles in the long term can create a localized calcium- and phosphorus-rich environment, which is favorable for osteogenesis [28, 39].

4. Conclusions

A simple method combining lyophilization with preheating treatment was adopted to produce asymmetric composite membranes from TCP and CS. In addition, the preheating time could be controlled to modulate the porosity and average pore size of the composite membranes, and in turn these structural factors could cause different behaviors in water absorption, enzymatic degradability and mechanical properties. The *in vitro* cell-culture using L929 fibroblasts proved that the composite membranes were non-toxic and had very good cell compatibility. The skin layer produced by preheating the solution for 40 min at 40°C could greatly enhance the mechanical modulus of the membrane and alleviate the extent of enzymatic degradation. Therefore, the skin layer could maintain a secluded space for the bone regeneration and prevent the potential invasion of other unwanted tissues. The porous layer produced by subsequent lyophilization exhibited an interconnected pore structure with high porosity and suitable pore size for the proliferation of hFOB1.19 osteoblast cells. Furthermore, the TCP particles incorporated into CS could further increase the rigidity and decrease the degradability of the membranes. Most importantly, the TCP particles were proved to increase the cell attachment and proliferation of hFOB1.19. Therefore, the TCPCS asymmetric composite membrane is a potential candidate as the barrier membrane for the periodontal treatment.

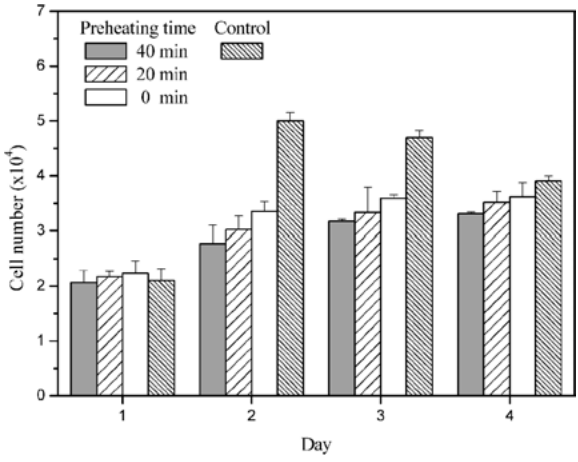

(a)

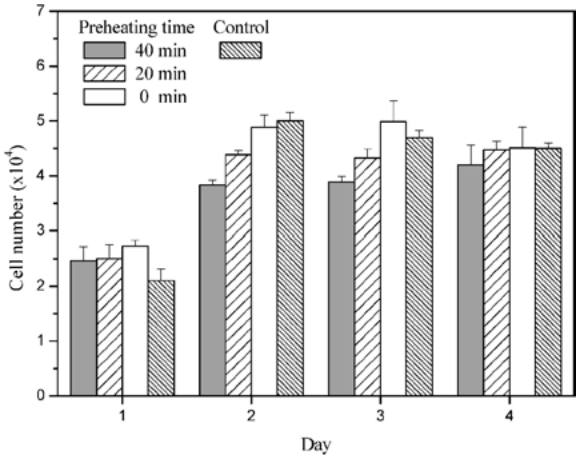

(b)

Figure 11. The proliferation of hFOB1.19 cells during 4 days of incubation on the porous layer of (a) CS membranes and (b) TCPCS membranes prepared with different preheating times before lyophilization.

Acknowledgement

The authors would like to thank National Science Council in Taiwan for the financial support.

References

1. P. Cortellini, G. Pini Prato and M. S. Tonetti, *J. Periodont.* **64**, 254 (1993).
2. C. Nublat, C. Braud, H. Garreau and M. Vert, *J. Biomater. Sci. Polymer Edn* **17**, 1333 (2006).
3. A. V. Imbronito, J. H. Todescan, C. V. Carvalho and V. E. Arana-Chavez, *Biomaterials* **23**, 4079 (2002).
4. J. Behring, R. Junker, X. Walboomers, B. Chessnut and J. Jansen, *Odontology* **96**, 1 (2008).
5. L. Jiang, Y. Li and C. Xiong, *J. Mater. Sci. Mater. Med.* **20**, 1645 (2009).

6. L. L. Hench, *J. Biomed. Mater. Res.* **41**, 511 (1998).
7. K. J. L. Burg, S. Porter and J. F. Kellam, *Biomaterials* **21**, 2347 (2000).
8. M. Kellomaki, H. Niiranen, K. Puumanen, N. Ashammakhi, T. Waris and P. Tormala, *Biomaterials* **21**, 2495 (2000).
9. O. Etienne, A. Schneider, C. Taddei, L. Richert, P. Schaaf, J. C. Voegel, C. Egles and C. Picart, *Biomacromolecules* **6**, 726 (2005).
10. P. A. Norowski, J. and J. D. Bumgardner, *J. Biomed. Mater. Res. B* **88**, 530 (2009).
11. S. H. Teng, E. J. Lee, P. Wang, D. S. Shin and H. E. Kim, *J. Biomed. Mater. Res. B* **87**, 132 (2008).
12. E. Nejati, H. Mirzadeh and M. Zandi, *Compos. A* **39**, 1589 (2008).
13. S. H. Teng, E. J. Lee, B. H. Yoon, D. S. Shin, H. E. Kim and J. S. Oh, *J. Biomed. Mater. Res. A* **88**, 569 (2009).
14. J. K. F. Suh and H. W. T. Matthew, *Biomaterials* **21**, 2589 (2000).
15. M. Rinaudo, *Prog. Polym. Sci.* **31**, 603 (2006).
16. K. Tomihata and Y. Ikada, *Biomaterials* **18**, 567 (1997).
17. V. Hamilton, Y. Yuan, D. A. Rigney, B. M. Chesnutt, A. D. Puckett, J. L. Ong, Y. Yang, W. O. Haggard, S. H. Elder and J. D. Bumgardner, *Polym. Int.* **56**, 641 (2007).
18. S. M. Lim, D. K. Song, S. H. Oh, D. S. Le-Yoon, E. H. Bae and J. H. Lee, *J. Biomater. Sci. Polymer Edn* **19**, 453 (2008)
19. L. Jiang, Y. Li, X. Wang, L. Zhang, J. Wen and M. Gong, *Carbohydr. Polym.* **74**, 680 (2008).
20. L. Wang and C. Li, *Carbohydr. Polym.* **68**, 740 (2007).
21. F. Zhao, Y. Yin, W. W. Lu, J. C. Leong, W. Zhang, J. Zhang, M. Zhang and K. Yao, *Biomaterials* **23**, 3227 (2002).
22. L. M. Mathieu, P.-E. Bourban and J.-A. E. Månson, *Compos. Sci. Technol.* **66**, 1606 (2006).
23. A. Afshar, M. Ghorbani, N. Ehsani, M. R. Saeri and C. C. Sorrell, *Mater. Des.* **24**, 197 (2003).
24. S. H. Kwon, Y. K. Jun, S. H. Hong and H. E. Kim, *J. Eur. Ceram. Soc.* **23**, 1039 (2003).
25. R. Z. LeGeros, *Chem. Rev.* **108**, 4742 (2008).
26. D. P. Link, J. van den Dolder, J. J. van den Beucken, J. G. Wolke, A. G. Mikos and J. A. Jansen, *Biomaterials* **29**, 675 (2008).
27. S. V. Madihally and H. W. T. Matthew, *Biomaterials* **20**, 1133 (1999).
28. T. L. Aronzeh, T. Tran, J. Mcalary and G. Daculsi, *Biomaterials* **26**, 3631 (2005).
29. V. Karageorgiou and D. Kaplan, *Biomaterials* **26**, 5474 (2005).
30. C. Y. Hsieh, S. P. Tsai, M. H. Ho, D. M. Wang, C. E. Liu, C. H. Hsieh, H. C. Tseng and H. J. Hsieh, *Carbohydr. Polym.* **67**, 124 (2007).
31. F. Liao, Y. Chen, Z. Li, Y. Wang, B. Shi, Z. Gong and X. Cheng, *J. Mater. Sci. Mater. Med.* **21**, 489 (2010).
32. S. M. Kuo, S. J. Chang, G. C.-C. Niu, C.-W. Lan, W. T. Cheng and C. Z. Yang, *J. Appl. Polym. Sci.* **112**, 3127 (2009).
33. T. M. Don, C. F. King and W. Y. Chiu, *J. Appl. Polym. Sci.* **86**, 3057 (2002).
34. T. M. Don and H. R. Chen, *Carbohydr. Polym.* **61**, 334 (2005).
35. T. M. Don, C. F. King and W. Y. Chiu, *Polym. J.* **34**, 418 (2002).
36. R. Zhang and P. X. Ma, *J. Biomed. Mater. Res.* **44**, 446 (1999).
37. H. S. Azevedo and R. L .Reis, in: *Biodegradable Systems in Tissue Engineering and Regenerative Medicine*, R. L. Reis and J. S. Román (Eds), Vol. 12, p. 179. CRC Press, Boca Raton, FL (2004).
38. A. Osorio-Madrazo, L. David, S. P. Trombotto, J. M. Lucas, C. Peniche-Covas and A. Domard, *Biomacromolecules* **11**, 1376 (2010).
39. I. D. Xynos, A. J. Edgar, L. D. K. Buttery, L. L. Hench and J. M. Polak, *J. Biomed. Mater. Res.* **55**, 151 (2001).